The Journal of Neuroscience, May 1989, 9(5): 1502–1515

Activation of $GABA_B$ Receptors Causes Presynaptic Inhibition at Synapses Between Muscle Spindle Afferents and Motoneurons in the Spinal Cord of Bullfrogs

Yan-yi Peng and Eric Frank

The Graduate Program in Neuroscience, Northwestern University, Evanston, Illinois 60201, and Department of Neurobiology, Anatomy and Cell Science, University of Pittsburgh Medical School, Pittsburgh, Pennsylvania 15261

Baclofen, a specific $GABA_B$ receptor agonist, was used to study the functional role of activation of $GABA_B$ receptors in synaptic transmission between muscle spindle afferents and motoneurons in the isolated spinal cord of bullfrogs. (±)-Baclofen (5 μM) reversibly reduced the amplitude of the excitatory postsynaptic potential (EPSP) evoked by simulation of various brachial muscle nerves and recorded extracellularly from the ventral root by 47% without shortening the falling phase of the EPSP. Neither the time course nor the amplitude of the action potentials in the sensory afferents was affected. Thus, baclofen caused synaptic inhibition without reducing either the potential change occurring in the muscle sensory afferents or the motoneuronal membrane resistance. Quantal analysis, performed using a deconvolution technique, of the monosynaptic EPSPs in brachial motoneurons evoked by activity in single triceps muscle spindle afferents showed that transmission at these synapses was quantal, and baclofen lowered the quantal content without altering the quantal size. Furthermore, quantal analysis of the electrical component of these unitary EPSPs showed that it did not fluctuate in amplitude, either in normal saline or with baclofen. The inhibition produced by activation of $GABA_B$ receptors is therefore presynaptic but is not likely to be caused by conduction failures in the sensory terminals.

Frank and Fuortes (1957) first suggested that conditioning stimuli to peripheral nerves could produce presynaptic inhibition of synaptic transmission between muscle afferents and motoneurons, the synaptic pathway that mediates the simple stretch reflex. Although the evidence remained either indirect or inconclusive for 30 years (reviewed by Burke and Rudomin, 1977; Nicoll and Alger, 1979), it has now been unequivocally demonstrated by quantal analysis of EPSPs elicited by activation of single sensory fibers that the inhibition is largely presynaptic (Clements et al., 1987). In addition to inhibition of the stretch reflex, electrical stimulation of sensory afferents in peripheral nerves causes depolarization of other primary afferents with a time course similar to that of the inhibition of the flexor reflex (Gasser and Graham, 1933; Hughes and Gasser, 1934; Barron and Matthews, 1938). Primary afferent depolarization (PAD) is produced primarily by GABA (Barker et al., 1975a, b), which also mediates synaptic inhibition pre- or postsynaptically in many systems. The close similarity in time course of PAD and the inhibition of the stretch reflex and the unaltered falling phase of the synaptic potential first led Eccles and his colleagues (Eccles et al., 1961) to postulate that PAD causes presynaptic inhibition of this reflex. The similarity of pharmacological effects has subsequently strengthened this view (reviewed by Nicoll and Alger, 1979).

In recent years, GABA has been found to activate 2 types of receptors in vertebrate neurons, i.e., $GABA_A$ and $GABA_B$ receptors (see review by Simmonds, 1983). $GABA_A$ receptors mediate the well-studied increase in chloride conductance (Bormann et al., 1987; Schofield et al., 1987), while $GABA_B$ receptors have been linked to either the blockade of voltage-gated Ca^{2+} channels (Dunlap, 1981; Dolphin and Scott, 1987) or increase in K^+ conductance (Gahwiler and Brown, 1985; Andrade et al., 1986; Howe et al., 1987).

Activation of either receptor type could conceivably result in the reduction of transmitter release from presynaptic terminals. In this study, we investigated the existence and the functional role of $GABA_B$ receptors at the synapses between muscle afferents and spinal motoneurons in the isolated spinal cord of bullfrogs. Our results show that activation of these receptors causes presynaptic inhibition without reducing the potential changes in muscle afferent terminals.

Materials and Methods

Dissection

Young adult bullfrogs (*Rana catesbeiana*), 4–6 cm long (Amphibians of North America, Nashville, TN) were anesthetized in ice water, decapitated, and eviscerated. The spinal cord was exposed by dorsal laminectomy. The choroid plexus, arachnoid, and dura were removed. For ventral root recordings, the following muscle nerves were dissected: medial, internal, external triceps, sternoradial, deltoid, suprascapular, and subscapular. For measurements of single unitary EPSPs the proximal and distal tendons of the medial head of the triceps brachii muscle were cut, and the muscle was dissected away from the surrounding tissue, keeping intact the nerve that innervates it. The nerve was carefully freed of connective tissue. The radial, ulnar, internal, and external triceps nerves were dissected as in the preparation for the ventral root recordings. The spinal cord was then transected at the level of the lumbar enlargement and hemisected longitudinally along the dorsal–ventral midline. For ventral root recordings, the root was cut where it joined the second DRG.

The preparation was bathed in oxygenated normal saline containing either 0 (i.e., no added) Mg^{2+} or 1 mM Mg^{2+} in a recording chamber at 14°C. The 0 Mg^{2+} saline contained (mM): Na^+, 116; K^+, 2; Ca^{+2}, 1.8; Cl^-, 122; glucose, 15; HEPES buffer, 5, at pH 7.2 (Frank and Westerfield,

Received July 18, 1988; revised Sept. 29, 1988; accepted Oct. 10, 1988.

We wish to thank Dr. Eugene M. Silinsky for his helpful comments on this study. This work was supported by NIH NS24373 to E.F.

Correspondence should be addressed to Yan-yi Peng at her present address: Department of Physiology, University of Pittsburgh Medical School, 3550 Terrace Street, Pittsburgh, PA 15261.

1982). The Mg^{2+} saline, in addition, had 1 mM $MgCl_2$. To compensate for the blocking effect of Mg^{2+} on synaptic transmission, an additional 1.8 mM $CaCl_2$ was added.

Ventral root recordings and intracellular recordings from motoneurons were made using either the 0 Mg^{2+} or the Mg^{2+} saline. In the 0 Mg^{2+} saline, cells had frequent bursts of spontaneous firing and the monosynaptic EPSPs often had late components that complicated the analysis of the time course of the falling phase of the potentials. The Mg^{2+} saline eliminated these complications without apparently altering the average amplitude, latency, or rise time of the chemical or electrical components nor the effects of baclofen on the monosynaptic EPSPs.

Electrophysiological recording techniques

Intracellular recordings were made with glass micropipettes (Omega dot tubing, Frederick Haer) filled with 2 M potassium methylsulfate with 0.5% Fast green added to aid visualization of the tip. The filled electrodes were beveled to have resistances between 15 and 40 MΩ using a micropipette beveler (K. T. Brown type BV-10, Sutter Instrument Co.). Extracellular recordings from ventral roots were obtained by placing the cut end of the root in a tightly fitting suction electrode. Changes in potential measured differentially between the suction electrode and the bath were recorded through an AC amplifier with high and low cut-off frequencies of 3 kHz and 0.1 Hz.

The stimulation strength to each individual peripheral nerve was 3.5 V, which is about 5 times the threshold and is suprathreshold for all the large-diameter muscle afferents. This stimulation strength was used to avoid the complications of differential recruitment of muscle afferent axons from trial to trial. In the Mg^{2+}-free saline, the frequent bursts of spontaneous firing required the use of low-frequency (2 Hz) stimuli and thus prolonged the time for collecting the number of traces necessary for analysis. In addition, it complicated the analysis of the time course of the falling phase of the potentials. Therefore, in later experiments, 1 mM Mg^{2+} saline was used with stimuli at 5 Hz, which was a low enough frequency that muscle spindles respond reliably to tapping but sufficiently high to make the collection of at least 2 sets of 1000 traces routine. To facilitate the comparison of intracellularly recorded EPSPs with the related population responses recorded from the ventral root, we used 5 Hz stimuli during ventral root recordings as well.

The experimental arrangement was the same as that used by Lichtman and Frank (1984). Action potentials in stretch-sensitive axons of the medial triceps nerve were recorded *en passant* using a hook electrode in mineral oil. Stretch-sensitive muscle afferents were activated by tapping the muscle surface at sensitive regions with a short length of straw fastened to a piezoelectric transducer. The straw was from a household broom and was coated with lacquer to make it waterproof. Individual muscle spindle afferents were activated by the straw tapper according to Lichtman and Frank (1984). Axons could follow these taps faithfully up to 20 Hz; a few of them followed up to 100 Hz.

The penetration and identification of motoneurons were made according to Frank and Westerfield (1982). Data were collected only for those motoneurons with an initial resting potential of at least −60 mV and a spike height of about 60 mV. As cells were routinely held for more than 40 min, and often for 1–2 hr, the measured resting potential tended to appear more negative than the initial measurement as evidenced by a negative shift in "zero" potential after withdrawal of the electrode from the cell. In order to compare the fluctuations of the monosynaptic unitary EPSPs (MUEPSPs) before and after application of drugs, it was crucial to maintain a stable resting potential. Therefore, several indirect criteria were used for this purpose. A set of traces was accepted only if the resting potential remained more negative than −60 mV and shifted by less than 5 mV during the measurement. In control experiments, the average MUEPSP amplitudes for 2 consecutive series of 1000 traces were within 20 μV of each other when the resting potential change was 5 mV or less.[1]

The piezoelectric tapper was activated at a fixed delay relative to the beginning of the recorded traces such that the extracellularly recorded muscle afferent spikes for a specific muscle unit occurred at approximately the same time in all the traces collected for the unit. This made it possible to obtain the averaged MUEPSPs during the experiment. The precise time of the spike was recorded for each trace so that the traces could subsequently be aligned more precisely. Furthermore, each trace was triggered at a fixed phase of the power line frequency, so that line frequency contamination could subsequently be removed mathematically (see below).

Pharmacological procedures

The preparations were bathed in about 23 ml of solution. The flow rate of superfusion was 3.3 ml/min. Thus, it took 7 min to change the entire bathing solution. However, as the spinal cord was situated between the inlet and outlet tubes, the rate of solution changes immediately around the preparation was probably faster than this.

For ventral root recordings, an average of the ventral root potential (VRP) evoked by stimulating all the triceps nerves or one of the other muscle nerves was obtained in normal saline. The perfusion solution was then switched to one containing 1, 5, 10, or 20 μM baclofen. One min after the superfusion of the drug solution began a series of averages of the VRPs were collected and the superfusion of the drug solution was continued for at least 10 min after the effects of the drug stabilized (details of the assessment of the effects of the drug are described in *Analysis of the data*). Drugs were then washed out by superfusing the preparation with normal saline and another series of averaged VRPs were recorded.

For studies of the MUEPSPs, 1000 traces were collected in control conditions as described above. Another 1000 traces were collected 4–20 min after the beginning of superfusion with saline containing 5 μM baclofen. If the resting potential of the motoneuron was stable after at least 10 min of washing out the drug and the averaged MUEPSP showed recovery, then a third set of 1000 traces was collected.

(±)-Baclofen was a gift from CIBA-Geigy Co. A stock solution (10^{-4}M) was made by first dissolving baclofen in 1 ml of 0.1 N HCl. The pH value of all solutions was adjusted to 7.2.

Analysis of the data

Data collection and analysis were carried out using an interactive BASIC (Indec) program run on a DEC 11/73 computer. The deconvolution procedure for quantal analysis used a FORTRAN program run on the same computer.

A typical VRP evoked by stimulating muscle afferents is shown in Figure 3*Aa*. The first sharp positive peak (arrow) is the afferent potential, a passive reflection of the action potentials in the sensory afferents. The second component, with a shape similar to the intracellularly recorded EPSP, is the extracellular equivalent of the population EPSP, that is, the EPSPs elicited by all muscle afferents of the stimulated nerve in all brachial motoneurons. Judged by its latency (3–6 msec), it was monosynaptic (Frank and Westerfield, 1982).

For the VRPs, the latency and peak amplitude of both the afferent and the monosynaptic potentials were analyzed. The halfwidth of the synaptic potentials was also measured. To facilitate visualization of any changes in the time course of the falling phase, the natural logarithm function of the VRPs was also plotted against time.

For the averaged intracellular recordings of the MUEPSPs (the averaging procedure is discussed below), the following parameters were analyzed: for the chemical component of the MUEPSP its (1) latency, (2) peak amplitude, (3) 0–100% rise time, (4) halfwidth, and (5) slope of the last linear portion of the semilogarithm trace of the falling phase. When the unit had an apparent electrical component, 2 additional parameters were measured: (1) the amplitude of the electrical component at the time the chemical component began and (2) the synaptic delay for chemical synaptic transmission, defined as the time between the beginning of the electrical component and the point when the chemical component started to rise. This operational definition gives an upper limit of the synaptic transmission time.

The 0–100% rise time was defined as the time interval between the points when the chemical component started and peaked. Because the averaged MUEPSPs were obtained from more than 600 traces that were synchronized by the action potential in a single muscle spindle afferent, the averaged traces had so little noise that the point where the chemical component began to rise could be easily identified. When there was an electrical component, this rise time was also measured on the natural logarithm traces since in many cases the break point between the elec-

[1] One series of MUEPSPs were analyzed while the resting potential was only −53 mV (b1 in Results). It was accepted for analysis because it was a unit with an electrical component of 240 μV and a peak chemical component of 1244 μV. This indicated that the penetration was good; bad penetrations are characterized by small noisy MUEPSPs and a rapid (< 10 min) decline of the resting potential. Also after superfusion of baclofen, the amplitude of the electrical component decreased only slightly and the slope of the natural logarithm of the last part of the falling phase remained the same.

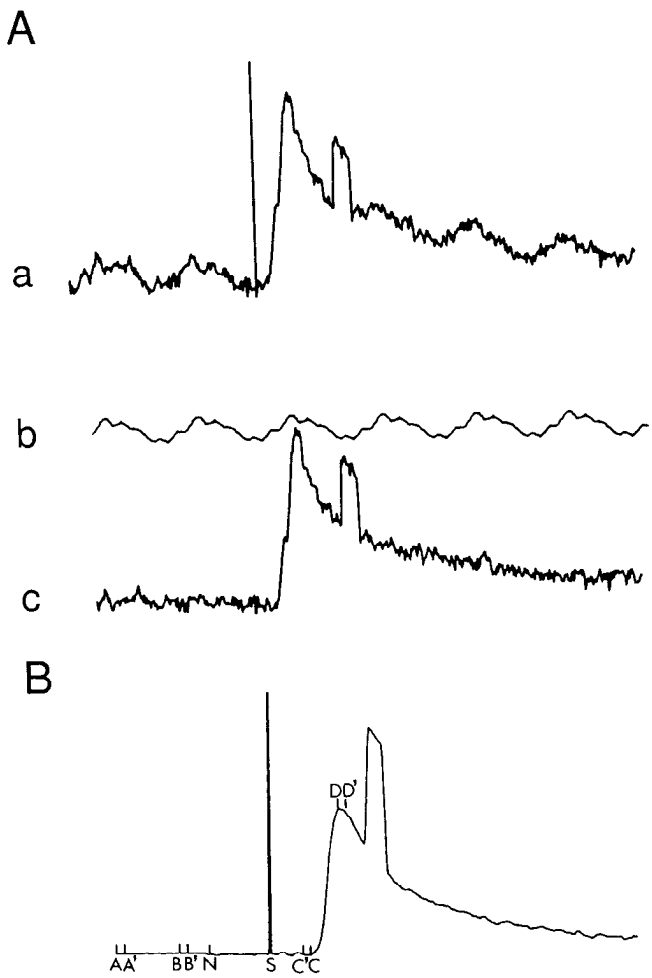

Figure 1. Method used to remove power line noise and to measure the peak amplitudes of MUEPSPs and noise in single traces. A raw single trace is shown in *Aa* (from MUEPSP unit b2 in Table 3) and was recorded at a fixed time relative to the power line frequency. The background noise was recorded at the beginning of each trace. Noises not phase locked to the power line frequency are eliminated by averaging; the resultant average over 1/60 sec (the segment corresponding to *AN* in *B*) therefore represents power line noise (*Ab*) and could be subtracted from each single trace. The resultant "cleaned" trace is shown in *Ac*. This was one of the worst examples of power line noise. Single "clean" traces were then temporally aligned with the nerve spike (*S* in *B*) and averaged (*B*, from unit b4 in Table 3). MUEPSP+noise was measured in single traces as the difference in amplitude between segment *DD'* and *C'C*, while the pure "noise" amplitude was measured for the corresponding time period *BB'* minus *AA'*. The calibration pulse on the falling phase of the MUEPSP is 0.5 mV and 2.5 msec. Because of the slight temporal shifting of the specific spike from trial to trial, the calibration pulse in *B* is wider at the base than at the top.

trical and chemical components and the point where the potential first reached its peak were more apparent than on the corresponding linear traces. In most cases, these 2 measurements gave similar results.

For each unit, the averaged EPSP was also plotted as the natural logarithm of the potential versus time. When MUEPSPs are generated by synapses located on distal dendrites or at different electronic lengths away from the recording site, the decay of the MUEPSP would not be a single-exponential function; therefore, its semilogarithm trace could not be fit by a single straight line (Rall, 1969). This was true for all the MUEPSP units that had peak amplitudes larger than 250 μV (see Fig. 5; for more examples, see Chap. 4, Peng, 1988). The membrane time constant of each cell was therefore the negative reciprocal of the slope of the last linear portion of the semilogarithm traces. For each unit, the slopes of this last linear portion with and without baclofen was compared.

Quantal analysis was used to study the fluctuation of the MUEPSPs in normal saline and baclofen. The large convergence of inputs to each spinal motoneuron makes an independent measurement of quantal size from the spontaneous miniature potentials impossible. Therefore, the traditional method of fitting the amplitude histogram to a Poisson or a binomial probability density function (pdf) is not appropriate. Instead, the deconvolution approach developed by Redman and his colleagues (Edwards et al., 1976; Wong and Redman, 1980) was used. This approach considers the experimentally measured signal as a linear summation of pure signal and noise (including potential changes caused by spontaneous release, evoked release due to spontaneous action potentials in various input pathways, and inherent noise of the recording system); therefore, the probability density function of the measured signal is a convolution of the probability density functions of the pure signal and pure noise. As the noise-contaminated signal and the noise can be measured independently, the probability density function of pure signal can be "deconvolved" from these 2 experimentally determined variables. (For a discussion of the rationale for the assumption of linear summation of signal and noise in frog spinal motoneurons refer to Chap. 3, Peng, 1988.)

The first step in this analysis, described in *I* below, is to measure the amplitudes of the individual MUEPSPs and the noise and thereby construct the probability density functions of these 2 variables. A quadratic optimization algorithm, described in *II*, is then used to deconvolve the pure MUEPSP probability density function from these data.

I. Measurements of the amplitudes of MUEPSPs and noise. Group the 2000 (or 3000, in the case of the MUEPSP units where a recovery set of data was collected) traces collected for a unit into 2 (or 3) sets, the control set and the experimental set (and a recovery set). For each set of traces, the following procedure was performed using an interactive program written in BASIC. The following description of the first part of the procedure is illustrated in Figure 1.

1. Select those traces that satisfy the following conditions: (a) an action potential in the spindle afferent occurred within ± 0.5 msec of the preset position of the action potential for this muscle sensory unit elicited by tapping the muscle unit, which was obtained while collecting the single traces. This action potential is called the specific action potential (S in Fig. 1*B*); (b) during an interval of 16.7 msec (1/60 sec, i.e., segment AN in Fig. 1*B*), which is prior to the activation of the tapper, there were no electronic artifacts or postsynaptic potentials produced by an action potential due to background activity in a medial triceps sensory axon; (c) no other action potentials recorded in the medial triceps nerve occurred before or after the specific action potential such that a monosynaptic EPSP elicited by that action potential could interfere with the part of the MUEPSP under study.

2. Average all the selected traces over the period corresponding to the AN segment in Figure 1*B*. Since each trace was phase-locked with the electrical noise of the power line, this averaging eliminated the random noise and resulted in the waveform of the line frequency contamination. An example of such a waveform is shown in Figure 1*Ab*.

3. Subtract the averaged power line noise in successive 16.7 msec segments from each of the selected raw traces to get "clean" traces. Figure 1*A* gives an example of this process.

4. Average the "clean" traces that are temporally aligned by their specific action potentials. An example of an averaged MUEPSP is shown in Figure 1*B*.

5. On the averaged trace define the window over which the peak amplitude of the MUEPSP was measured. Set a window (segment DD' in Fig. 1*B*) at the peak of the averaged MUEPSP and a cursor at the point (point C in Fig. 1*B*) where the MUEPSP started (for details see Chap. 2, Peng, 1988).

6. For each "clean" trace, measure the amplitudes of the MUEPSP as the difference between the average potential in DD' and in C'C, and the amplitude of the noise as the difference between the 2 corresponding periods in the initial portion of the trace (BB' minus AA'). Calculate the mean value and the SD for the amplitudes of MUEPSPs and noise.

7. Make one histogram from each set of MUEPSP and noise amplitude files (see example in Fig. 2, *A, B*). Three additional histograms of the MUEPSP amplitudes were made with the lower limit of each bin shifted to the left by a fraction of the bin width (Edwards et al., 1976). For each MUEPSP unit, the binwidth was first chosen to be 1 SD of the noise (1 σ_n). If the results of the subsequent deconvolution procedure (see *II* below) generated a good statistical fit to the data yet the separation

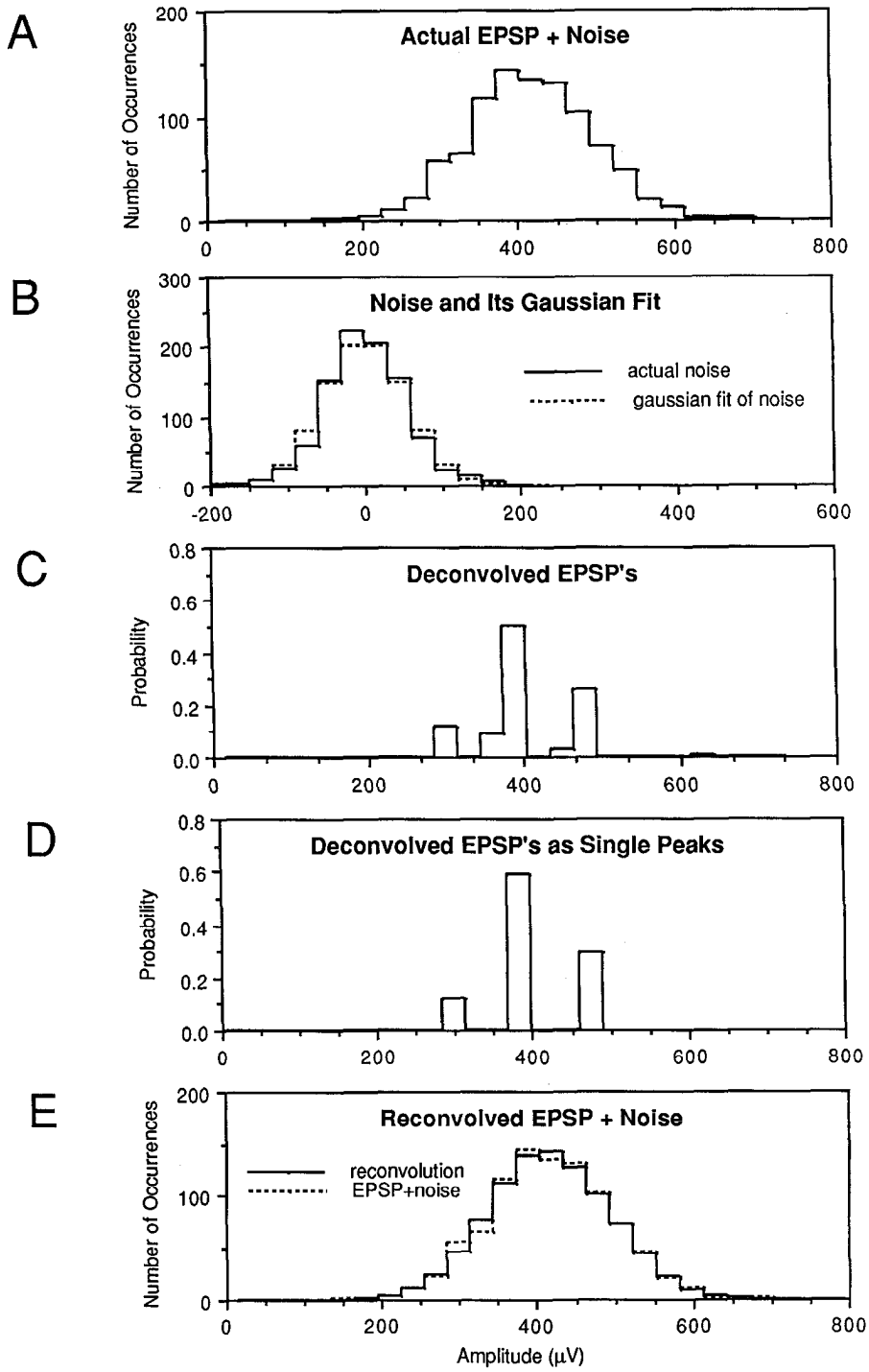

Figure 2. An example of the deconvolution procedure. *A,* Amplitude histogram of recorded MUEPSP amplitudes (including noise) measured as described in Figure 1. *B,* Amplitude histogram of recorded noise measured during the initial portion of each trace. A Gaussian fit of this distribution is also shown, and was used for the subsequent analysis. *C,* Probability density function of the pure MUEPSPs deconvolved from the distributions shown in *A* and *B. D,* Adjacent nonzero bins have been combined (see text for details), and bins with a probability of less than 0.01 have been deleted. All histograms in this and the subsequent paper have been simplified in this manner. *E,* Reconvolution of the pure MUEPSPs and the noise. The histogram of the recorded MUEPSPs (from *A*) has been superimposed for comparison.

between adjacent nonzero bins was not clear then the binwidth was reduced to 0.5 σ_n and another run of the deconvolution was repeated. The results of the second run were accepted only if the statistical fit of the results to the experimental data was not made worse by this reduction in binwidth. The lower limit of the bin size was chosen as 0.5 σ_n because of the performance of the deconvolution algorithm on simulated data (see below).

II. The deconvolution procedure. The pure MUEPSP pdf was then deconvolved from the noise and MUEPSP + noise histograms using a quadratic optimization algorithm devised by Fletcher (1970, 1971). The computer program was based on the one described by Wong and Redman (1980), kindly provided by Dr. R. F. Edwards. A subroutine that tests whether or not the Hessian matrix of the objective function of the optimization procedure was positive definite was added (for mathematical rationale and numerical details see Chap. 3, Peng, 1988). For each histogram, 3 deconvolutions were performed: (a) between the raw noise pdf and the noise-contaminated signal pdf, (b) between the raw noise and the Gaussian fit of the noise, and (c) between the noise-contaminated signal pdf and this Gaussian fit of the noise (Wong and Redman, 1980). An example of the last type of deconvolution is shown in Figure 2*C*.

Usually this deconvolution procedure resulted in pairs of adjacent nonzero bins separated from other pairs by one or more zero bins (as in Figure 2*C*). Because isolated amplitude bins were frequently split into 2 adjacent nonzero bins when the deconvolution procedure was tested with simulated data (see below), we combined such pairs into a

Table 1. Results of deconvolution when simulations used experimental noise data

P_x	σ_n (μV)	Sample size (n)	Binwidth (μV)	p_x	p_{χ^2}
$P_{100\mu V} = 1$	40	50	25	$p_{100\mu V} = 1$	100
$P_{100\mu V} = 0.5$				$p_{100\mu V} = 0.499$, $p_{0\mu V} = 0.001$	
$P_{200\mu V} = 0.5$	50	800	50	$p_{200\mu V} = 0.5$	>0.995
$P_{100\mu V} = 0.5$				$p_{100\mu V} = 0.5$	
$P_{150\mu V} = 0.5$	50	800	50	$p_{150\mu V} = 0.5$	>0.995
$P_{100\mu V} = 0.7$				$p_{100\mu V} = 0.6905$, $p_{75\mu V} = 0.0045$	
$P_{200\mu V} = 0.3$	50	800	25	$p_{200\mu V} = 0.2979$, $p_{175\mu V} = 0.0053$	>0.995
				$p_{225\mu V} = 0.0015$	
$P_{100\mu V} = 0.7$				$p_{100\mu V} = 0.6976$, $p_{50\mu V} = 0.0019$	
$P_{150\mu V} = 0.3$	50	800	25	$p_{150\mu V} = 0.3004$	>0.995
$P_{100\mu V} = 0.3$				$p_{100\mu V} = 0.2963$, $p_{125\mu V} = 0.0041$	
$P_{200\mu V} = 0.3$				$p_{200\mu V} = 0.2979$, $p_{225\mu V} = 0.0039$	
$P_{300\mu V} = 0.4$	50	800	25	$p_{300\mu V} = 0.3974$, $p_{325\mu V} = 0.0007$	>0.995
$P_{100\mu V} = 0.3$				$p_{100\mu V} = 0.2862$, $p_{125\mu V} = 0.0416$	
$P_{150\mu V} = 0.3$				$p_{150\mu V} = 0.2333$, $p_{175\mu V} = 0.0663$	
$P_{200\mu V} = 0.4$	50	800	25	$p_{200\mu V} = 0.3592$, $p_{225\mu V} = 0.0131$	>0.995
$P_{100\mu V} = 0.3$				$p_{100\mu V} = 0.2993$, $p_{125\mu V} = 0.001$	
$P_{175\mu V} = 0.3$				$p_{175\mu V} = 0.3005$	
$P_{250\mu V} = 0.4$	50	800	25	$p_{250\mu V} = 0.3976$, $p_{275\mu V} = 0.0014$	>0.995
$P_{100\mu V} = 0.7$				$p_{100\mu V} = 0.6765$, $p_{75\mu V} = 0.0122$	
$P_{175\mu V} = 0.1$				$p_{175\mu V} = 0.0758$, $p_{150\mu V} = 0.0304$	
$P_{250\mu V} = 0.2$	50	800	25	$p_{250\mu V} = 0.1915$, $p_{225\mu V} = 0.0133$	>0.995
				$p_{25\mu V} = 0.007$	
$P_{100\mu V} = 0.2$				$p_{100\mu V} = 0.1985$, $p_{150\mu V} = 0.0049$	
$P_{200\mu V} = 0.2$				$p_{200\mu V} = 0.1819$, $p_{250\mu V} = 0.0012$	
$P_{300\mu V} = 0.2$				$p_{300\mu V} = 0.1815$, $p_{325\mu V} = 0.0137$	
$P_{400\mu V} = 0.4$	50	800	25	$p_{400\mu V} = 0.2925$, $p_{425\mu V} = 0.0061$	>0.995
$P_{400\mu V} = 0.2$				$p_{400\mu V} = 0.199$	
$P_{500\mu V} = 0.2$				$p_{500\mu V} = 0.202$	
$P_{600\mu V} = 0.2$				$p_{600\mu V} = 0.197$, $p_{630\mu V} = 0.001$	
$P_{700\mu V} = 0.2$				$p_{700\mu V} = 0.2$	
$P_{800\mu V} = 0.2$	55.12	803	33	$p_{800\mu V} = 0.195$, $p_{830\mu V} = 0.005$	>0.995

The simulations were grouped according to the number of the nonzero probable bins to be resolved. The groups are separated by solid lines, whereas each simulation is separated by dotted lines. $P_{x\mu V}$ denotes the given probability of events in a bin whose mean is $x\mu$V, and $p_{x\mu V}$ for the equivalent probability resulting from the deconvolution procedure. The SD of the noise is denoted as σ_n. p_{χ^2} is the probability for the histogram (resulted from the convolution of the results of deconvolution procedure with noise pdf) to be a random sample from the originally simulated histogram based on the χ^2 statistics.

single bin whose mean was the weighted average of the pair and whose probability was the sum of those of the adjacent bins, as illustrated in Figure 2*D*.

The reliability of the deconvolved "pure" MUEPSP pdf was tested by reconvolving it with the noise. Figure 2*E* shows the good agreement obtained between this reconvolution and the original MUEPSP + noise data. In most cases the goodness of fit of the reconvolved MUEPSP + noise histogram with that of the experimental data was tested by a χ^2 test. The results were accepted only if the confidence level of this test was better than 95%. When the χ^2 test was not appropriate (i.e., more than 20% of the bins had a frequency of occurrence of less than 5, see Hays, 1973), the Kolmogorov-Smirnov test was used instead (Smirnov, 1948; Massey, 1951).

Testing of the deconvolution algorithm by simulated data

The performance of the quadratic optimization algorithm was tested using simulated data. The simulated data were generated in 2 ways. For each test a pure signal pdf was constructed with 1–5 amplitude bins each with a specific nonzero probability of occurrence. This discrete probability density function was then convolved with the experimental noise probability density function, or a random noise probability density function with the same range of SDs as that of the empirical noise data. The randomization was made using a Monte Carlo method (Shreider, 1966). The results of deconvolution for these simulated data are listed in Tables 1 and 2.

1. Simulated data with experimental noise. As shown in Table 1, when there was one nonzero bin, the algorithm resolved it in one iteration with $\chi^2 = 0$ for sample sizes between 50 and 800. When there were 2–5 nonzero bins separated by 1–2 σ_n, the algorithm resolved all the given nonzero bins with negligible error. For these simulations the sample size was 800 and the binwidth was 0.5–1 σ_n.

2. Simulated data with randomly generated noise. The finite sample size used for generating the random noise and the noise-contaminated signal histograms introduced some errors in the deconvolution procedure. As the third simulation in Group I (Table 2) illustrates, the good-

Table 2. Results of deconvolution when simulations used random noise with given σ_n

P_x	σ_n (μV)	Sample size (n)	Binwidth (μV)	p_x	p_{χ^2}
$P_{100\mu V} = 1$	41.3	800	25	$p_{100\mu V} = 0.988$, $p_{125\mu V} = 0.012$	>0.975
$P_{100\mu V} = 1$	64.99	829	33	$p_{99\mu V} = 0.929$, $p_{132\mu V} = 0.071$	>0.95
$P_{100\mu V} = 1$	64.99	400	33	$p_{99\mu V} = 0.977$, $p_{66\mu V} = 0.023$	~0.25
$P_{100\mu V} = 0.5$ $P_{200\mu V} = 0.5$	50	829	33	$p_{66\mu V} = 0.056$ $p_{99\mu V} = 0.447$ $p_{165\mu V} = 0.014$ $p_{198\mu V} = 0.455$ $p_{264\mu V} = 0.028$	>0.75
$P_{180\mu V} = 0.5$ $P_{360\mu V} = 0.5$	60	800	30	$p_{168\mu V} = 0.099$ $p_{198\mu V} = 0.397$ $p_{348\mu V} = 0.117$ $p_{378\mu V} = 0.334$, $p_{438\mu V} = 0.052$	>0.90
$P_{100\mu V} = 0.4$ $P_{200\mu V} = 0.3$ $P_{300\mu V} = 0.3$	50	800	25	$p_{100\mu V} = 0.36$, $p_{125\mu V} = 0.039$ $p_{200\mu V} = 0.319$ $p_{300\mu V} = 0.144$, $p_{325\mu V} = 0.139$	>0.975
$P_{100\mu V} = 0.4$ $P_{200\mu V} = 0.3$ $P_{300\mu V} = 0.3$	50	900	25	$p_{70\mu V} = 0.048$ $p_{95\mu V} = 0.338$, $p_{120\mu V} = 0.027$ $p_{195\mu V} = 0.11$, $p_{220\mu V} = 0.151$ $p_{295\mu V} = 0.31$, $p_{320\mu V} = 0.016$	>0.99

The simulations are grouped the same way as in Table 1. $P_{x\mu V}$, $p_{x\mu V}$, σ_n, and p_{χ^2} are used as in Table 1.

ness of fit of the results of deconvolution was made worse when the sample size was small. Despite the occurrence of erroneous bins, all the real nonzero bins (the number of the nonzero bins varied from 1 to 3) were resolved, and the erroneous bins had a much smaller probability. When the bins were divided such that the given nonzero bins were not located at the mean value of the bins used for deconvolution, the nonzero bin tended to split into 2 adjacent bins, as illustrated in the second simulations in groups II and III (Table 2). Because of this possibility, in analyzing experimental data, 4 different histograms were routinely constructed for each MUEPSP unit for 4 different positions of the bins, and deconvolution was carried out for each of these 4 histograms. Notice that in the 2 examples given in group II, an additional nonzero bin with small probability occurred and it is separated from the dominant "real" bins by one zero bin. These results showed that bins with probabilities less than 0.05 are likely to be unreliable, and we have not used them in calculating quantal sizes.

Rationale for adopting the quadratic optimization algorithm for the deconvolution procedure instead of a simplex method

The main criticism against applying the Fletcher algorithm for optimization is statistical. Different statistical criteria of fitness have been used to construct the objective function for optimization, for example, the sum of square error, χ^2 value, and the maximum likelihood estimator (MLE). Theoretically, the sum of square error is inferior to the other 2 criteria since it does not take the proportionality of the error relative to its expected value into account. In an empirical study, Ling and Tolhurst (1983) compared the Newton-Raphson optimization algorithm with a simplex algorithm based on each of the above 3 criteria for statistical fitness. They found that all criteria and optimization algorithms yield results with errors within a physiologically tolerable range. However, when the sample size was less than 400, the sum of square errors was the least reliable statistically. The performance of the Newton-Raphson method using the sum of square errors as the criterion of fitness is most sensitive to increase in sample size, and when it is near 800, the reliability of this method is similar to the other 2 criteria using the simplex algorithm.

The quadratic algorithms are superior to the simplex algorithms in 2 respects. First, they can distinguish the global minimum from local ones. The minimum found by a simplex algorithm is only a local one and may therefore be influenced by the chosen initial solution. Indeed, Hosmer (1978) reported that the MLE algorithm converges to different answers depending on which starting values were employed. Ling and Tolhurst (1983), however, found that when the simplex method did converge, the choice for the initial values was not relevant. Second, quadratic algorithms have quadratic convergence, whereas simplex algorithms have linear convergence. Ling and Tolhurst (1983) reported that 10 (occasionally 20) iterations were adequate for the estimates to stabilize to 3 significant figures (similarly, we found that for a search in 30- to 40-dimensional spaces, it usually took fewer than 20 iterations for the Fletcher algorithm to converge), whereas a solution using the MLE with a simplex algorithm usually required 50–200 iterations. This makes the simplex algorithm impractically time-consuming if performed on a laboratory microcomputer. Furthermore, the Fletcher algorithm is faster than the simple Newton-Raphson method evaluated by Ling and Tolhurst (1983) because instead of calculating the search vectors at each iteration, the Fletcher algorithm only updates them (see Chap. 3 in Peng, 1988, for details).

Based on these theoretical reasons, on the adequate performance of the Fletcher algorithm for our simulated data and on our relatively large sample sizes (600–950), we chose to use the sum of square error as the fitness criterion and the Fletcher algorithm to carry out the deconvolution procedure.

Results

Inhibition of population EPSPs by baclofen

Ventral root recording is a nonintrusive method of studying the population response of spinal cord motoneurons. It was used to study whether $GABA_B$ receptors are present at muscle afferents and/or spinal cord motoneurons, and if they are present, how they affect the synaptic input from the muscle sensory afferents.

Baclofen reduced the peak amplitudes of the monosynaptic component of the VRPs. On average, the reduction of the triceps-VRPs was 31.6% ($n = 2$) for 1 μM, 47% ($n = 8$) for 5 μM, 56%

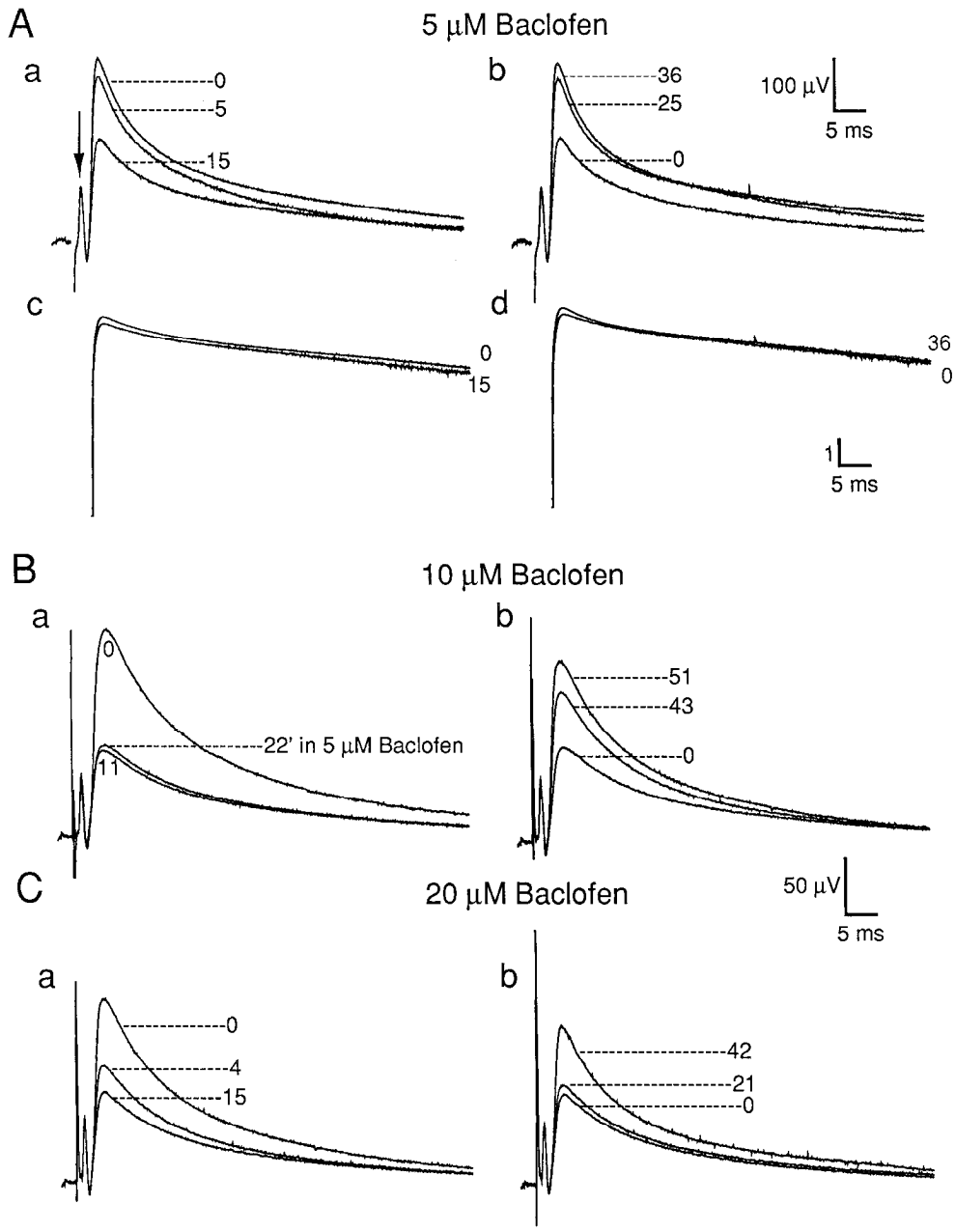

Figure 3. Time course, amplitude, and dose dependence of the effects of baclofen on triceps-VRPs. *A–C,* Effects of 5, 10, and 20 μM baclofen on triceps-VRPs (*left-hand traces*) and the recovery from the effect after washing the preparation with normal saline (*right-hand traces*), respectively. Traces in panels *c* and *d* are semilogarithmic plots of the traces in *a* and *b,* respectively. The baselines have been shifted to facilitate comparison of the falling phases. The numbers on the traces refer to minutes in baclofen for *a* and *c* and after return to normal saline for *b* and *d.* The *arrow* in *Aa* points to the afferent potential.

(n = 2) for 10 μM, and 53% (n = 1) for 20 μM baclofen. The blockade was reversible as demonstrated by the right-hand traces in Figure 3. The monosynaptic component of VRPs elicited by other muscle afferents (sternoradialis, deltoid, and subscapularis) was similarly reduced (49% reduction by 5 μM baclofen, n = 5). This reduction was dose dependent up to 10 μM and then saturated (Fig. 4*A*).

The monosynaptic component of the VRP is the extracellular equivalent of the average monosynaptic EPSP in all motoneurons with an axon in the 2nd root evoked by stimulation of a specific muscle nerve. The fact that baclofen inhibited these VRPs indicated that $GABA_B$ receptors exist either on the muscle afferents, on motoneurons or on both.

Baclofen did not shorten the falling phase of the VRPs. This was studied using both the slope of the falling phase of the semilogarithm traces of the VRPs and the halfwidth of the averaged VRPs. The semilogarithm traces in Figures 3*Ac* and 4*B* show that baclofen did not increase the slopes of the falling phase of these VRPs, indicating that the time constants of the decay phase of these potentials were not decreased. Because these slopes are largely determined by the time constant of the motoneuronal membrane, these findings suggest that the inhibition by baclofen is not accompanied by a measurable increase in membrane conductance of the motoneurons. In fact, there was a slight increase in these time constants. This phenomenon was similarly reflected by measurements of halfwidth. Indeed, at 5, 10, and 20 μM, baclofen increased, rather than decreased, the halfwidth of the triceps-VRPs by 3.5% (n = 2), 17.5% (n = 2), and 22% (n = 1), respectively. Similarly, 5 μM baclofen increased the halfwidth of the VRPs evoked by stimulating the sternoradial, deltoid, and subscapular nerves by 5% (n = 3).

Baclofen had no effect on the amplitude and time course of the afferent potentials. The afferent potential, which is the first deflection after the stimulation artifact, was completely un-

changed by any of the concentrations of baclofen used (1–20 μM). This is illustrated in the traces in Figure 3. The absence of change in afferent potentials suggests that the inhibition produced by baclofen is not the result of a detectable reduction in the number of active sensory fibers or in the magnitude of the sensory impulses themselves.

Effects of baclofen on intracellularly recorded averaged MUEPSPs

The effect of baclofen on synaptic transmission between individual muscle afferents and motoneurons was studied in 17 cases, where 1000 traces of intracellularly recorded MUEPSPs were obtained both before and after the superfusion with baclofen. These MUEPSP units are arbitrarily categorized as big, medium, or small according to their peak amplitudes. The big units had peak amplitudes greater than 500 μV, the medium units had peak amplitudes between 250 and 500 μV, and the small units had peak amplitudes below 250 μV. There are 7 big units, 4 medium units, and 6 small units. Data for these units are presented in Tables 3 and 4. The traces of the averaged MUEPSPs for 3 units are shown in Figure 5.

Several conclusions can be made based on the averaged MUEPSP traces.

Baclofen inhibited the amplitude of MUEPSPs. Similar to the results from ventral root recordings, 5 μM baclofen reduced the amplitude of the MUEPSPs in 6 of 7 big units and all medium and small units (3 examples are illustrated in Fig. 5; also see Table 3). The reduction ranged from 11 to 68% (mean = 36.5%, SD = 16%). Partial recovery was observed for 7 of the units where the recording remained stable enough after washing out baclofen with normal saline solution for more than 20 min so that another set of 1000 traces could be recorded (for examples, see Fig. 5, *A, C*; also see Table 3).

The sets of traces for the baclofen effect were taken beginning 4–10 min (for unit m3 only the first baclofen set of data is considered) after the superfusion of baclofen had started. Since the effect of baclofen plateaued after ~13 min, for this range of superfusion time the full effect of baclofen might not have been achieved when the data were collected. However, no significant correlation was found (R = 0.025, degree of freedom = 14) between the time in baclofen and the amount of resulting inhibition. The large variability in amount of inhibition observed in different units is therefore likely to be due to other factors.

The amplitude of unit b6 increased in the presence of baclofen. However, this unit had other abnormal properties as well (see below).

Baclofen had relatively little effect on the time course of the MUEPSPs. In 14 of the 17 units studied, the latency between the time of the sensory impulse recorded in the medial triceps nerve and the beginning of the MUEPSP was not altered by baclofen. This is apparent in the averaged traces in Figure 5 (also see Fig. 10, Peng, 1988). In another 2 units (s3 and s4), the latency was somewhat increased, while for unit b6 the latency was decreased. A possible explanation for these 3 cases is that the bath temperature may have changed during superfusion with baclofen, which would alter the conduction velocity. The increase in MUEPSP amplitude and decrease in synaptic delay and rise time (see below) for unit b6 would be consistent with such a change. In any case, there was no consistent effect of baclofen on latency.

Baclofen did not change the synaptic delay, as documented in Table 3. For 12 units there was an early electrical component

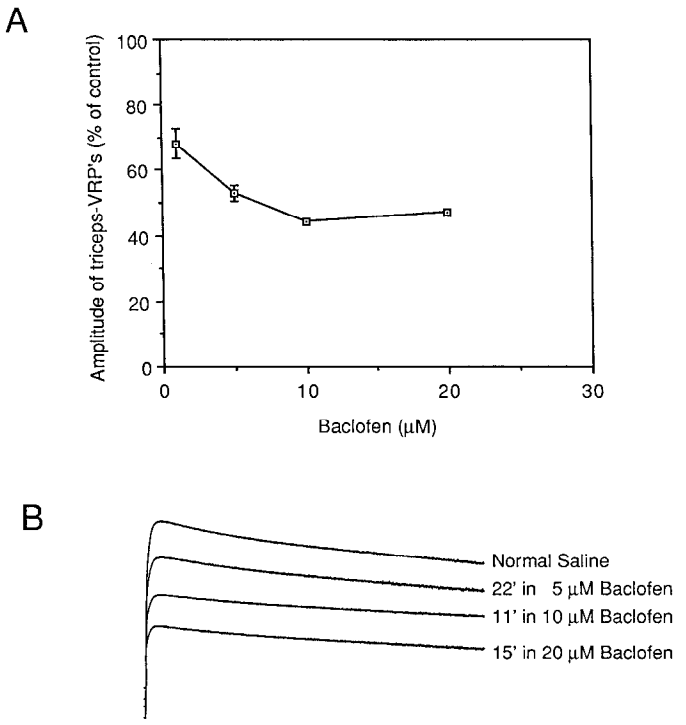

Figure 4. *A,* Dose–response curve of the effect of baclofen on inhibition of the peak amplitude of the triceps-VRPs. The error bars show SEM. *B,* Semilogarithmic traces of triceps-VRPs in normal saline and after the effects of 5, 10, and 20 μM baclofen reached their plateau. The baselines have been shifted to facilitate comparison of the falling phases.

of the MUEPSP, which makes it possible to measure the synaptic delay quite precisely (see Materials and Methods). The delay in the presence of baclofen was within 0.2 msec of the control value for 11 of these units, and the last unit was within 0.3 msec, which is probably within the error of measurement. This result is consistent with those from the ventral root recordings (refer to Fig. 3).

Baclofen had virtually no effect on the rise time of the MUEPSPs of 10 units (allowing 0.3 msec as measurement error), and it decreased the rise time for the other 7 units (see Table 3). There was no significant correlation (R = 0.09, df = 14) between the percentage reduction in rise time and the percentage inhibition of MUEPSP amplitude caused by baclofen.[2]

The falling phase of an EPSP is a sensitive indicator of the postsynaptic membrane time constant, as well as the location of the synaptic sites responsible for the EPSP. It was analyzed by measuring both the MUEPSP halfwidth and the slope of the semilogarithm plot of the falling phase. For the small units the falling phase of the semilogarithm traces of MUEPSPs could be fit by a straight line, whereas for the medium and big units at least 2 straight lines were required. The lines that fit the earlier part of the falling phase had a more negative slope than that for the later part, as predicted by a mathematical model proposed for spinal cord motoneurons (Rall, 1969). The negative reciprocal of the slope of the last linear portion of the semilogarithm traces is the time constant of the membrane. In all of the 17 units the absolute value of this slope was not increased in bac-

[2] When the MUEPSP unit had a measurable early electrical component, the amplitude of the chemical component was defined as the difference between the late and the electrical components.

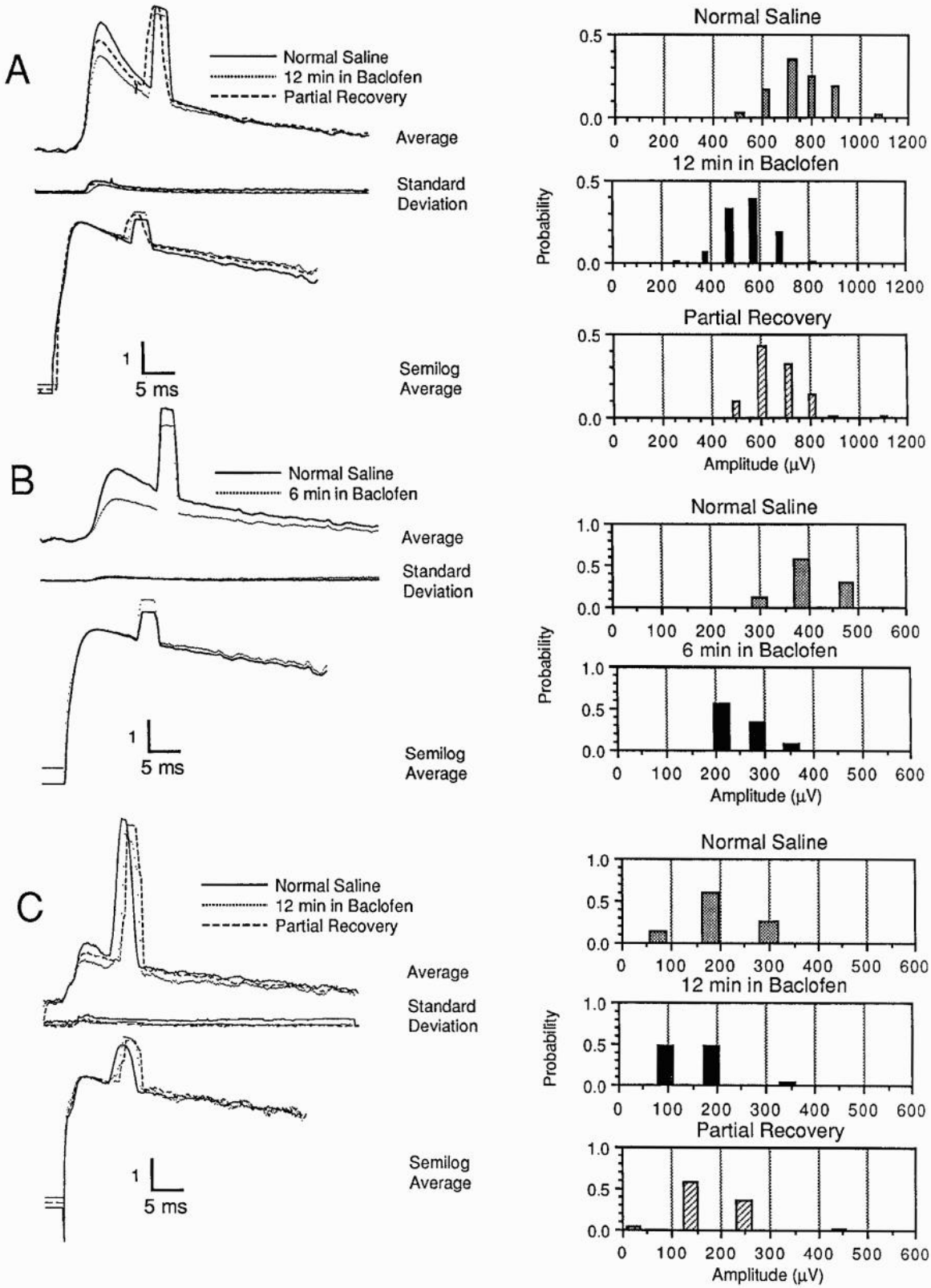

Figure 5. Effect of 5 μM baclofen on MUEPSPs. Three units are shown: *A*, unit b3 (as listed in Table 3); *B*, unit ml; and *C*, unit s2. The peaks of the semilogarithmic traces for each MUEPSP unit have been superimposed to facilitate the comparison of their slopes. The calibration pulses on the falling phase of the averaged MUEPSP traces are 0.5 mV. The results of the deconvolution procedure for these units are shown on the *right*.

Table 3. Effects of 5 μM baclofen on MUEPSPs

Unit	Solution	Sample size (*n*)	Amplitude ele/late (μV)	Amplitude$_{ele}$ % of control	Amplitude$_{chem}$[a] % of control	Synaptic delay (msec)	Rise time ave/ln (msec)	Halfwidth (msec)	Halfwidth % of control	Quantal size (μV)	Bin-width (μV)
b1	Saline	808	186/1244			1.5	1.6/1.7	5.2		162	50
	Baclofen	683	172/936	92.5	72.2	1.5	1.5/1.5	3.4	65	150	50
b2	Saline	692	521/1474			1.9	1.9/1.8	9.0		150	50
	Baclofen	723	375/946	72	59.9	1.9	1.9/1.7	4.4	48.9	125	50
b3	Saline	803	84/741				3.4/3.2	10.8		92	30
	Baclofen	755	102/535	121	65.9		3.1/3.1	13.8	127.8	101	25
	Saline	719	91/644	108	84.2		3.3/3.4	12.6	116.7	103	30
b4	Saline	929	46/592			1.3	3.5/4.1	11.9		122	33
	Baclofen	855	30/334	65	55.7	1	3.7/?	11.1	93.3	106	30
b5	Saline	620	119/707			1.6	3.1/3.6	16.1		154	33
	Baclofen	406	120/308	101	32.0	1.6	3.2/?	19.7	122.4	118	33
b6	Saline	791	114/491			3.2	4.7/4.3	12.3		135	30
	Baclofen	831	153/626	134	125.5	3.2	2.8/2.9	10.1	82	136	30
b7	Saline	784	176/520			1.8	2.0/1.9	13.7		121	33
	Baclofen	823	173/422	98	72.4	1.7	1.5/1.5	16.5	120.4	116	33
m1	Saline	942	56/424			2	5.1/5.1	20.4		88	30
	Baclofen	835	42/240	75	53.8	2	4.3/4.0	24.2	118.6	71	30
m2	Saline	705	161/416			1.8	2.1/2.3	16.5		115	33
	Baclofen	747	160/298	99	54.1	1.6	2.3/2.3	20.4	123.6	95	25
	Saline	705	155/341	96	72.9	2.2	2.1/2.3	20.6	125	102	33
m3	Saline	779	88/339			2.1	2.8/2.5	8.8		115	33
	1st baclofen	828	90/304	102	85.3	2	2.7/2.5	9	102		
	2nd baclofen	869	65/253	74	74.9	2	2.5/3.0	8.6	98	125	50
m4	Saline		/335				4.4/4.1	43.9			
	Baclofen		/218		65.1		3.8/3.7	41.3	94		
	Saline		/262		78.2		3.6/?	42.4	96.6		
s1	Saline	742	29/235			1.6	3.3/3.2	20.5		116	33
	Baclofen	788	28/211	97	88.8	1.6	3.2/3.2	22.5	109.8	121	33
s2	Saline	711	58/203			2.2	2.6/2	16.5		96	
	1st baclofen	784	58/163	100	72.4	2.2	1.9/2	15.8	95.8	90	30
	2nd baclofen	831	63/148	109	58.6	2.2	2.6/2.2	18.5	112	91	30
	Saline	833	63/178	109	79.3	2.1	2.0/1.9	23	139.4	108	30
s3	Saline	613	/183				4.5/4.5	17.1		77	25
	Baclofen	805	/90		49.2		4.2/2.9	24.1	141	80	20
	Saline	935	/121		66.1		5.2/?	26.3	153.8	75	25
s4	Saline	733	/120				5.5/5	20.6		100	25
	Baclofen	710	/76		63.3		4.6/4.3	20.5	100	100	25
s5	Saline	783	/56				3.2/3.3	34.1		65	25
	Baclofen	770	/21		37.5		2.5/?	?	?	65	25
	Saline	754	/50		89.3		3.7/3.4	39.5	115.8	67	25
s6	Saline	767	28/92			1.6	2.4/?	13.9			
	Baclofen	746	35/85	125	78.1	1.4	2.2/2.3	14.4	103.6		
	Saline	787	36/92	129	87.5	1.6	2.4/?	15.9	114.4		

ele, electrical; chem, chemical; ave, average; ln, natural logarithm. ? indicates when it was not possible to make an accurate measurement.

[a] When the MUEPSP unit had an early electrical component, the amplitude of the chemical EPSP was defined as the difference between the amplitudes of the late and the electrical components.

lofen. If the drug did not affect the capacitance of the membrane (which is likely), this result indicates that baclofen did not increase motoneuronal membrane conductance. In fact, for 5 units (b3, b5, m1, m2, and s6), the absolute value of this slope decreased slightly, suggesting an increase in motoneuronal membrane time constant and hence a possible decrease of motoneuronal membrane conductance.

In 14 of the 17 units the slope of the initial portion of the falling phase (plotted in semilog coordinates) was also not altered by baclofen. However, in 2 units (b1 and b2), this slope was more negative in baclofen. A similar phenomenon occurred for unit b6 to a much lesser degree. The increase of the absolute value of this slope in these 3 units was mirrored in the halfwidth measurements. In baclofen the halfwidths for units b1, b2, and b6 were decreased by 35, 51.2, and 18%, respectively. In contrast, baclofen decreased the halfwidth of 3 other units by less

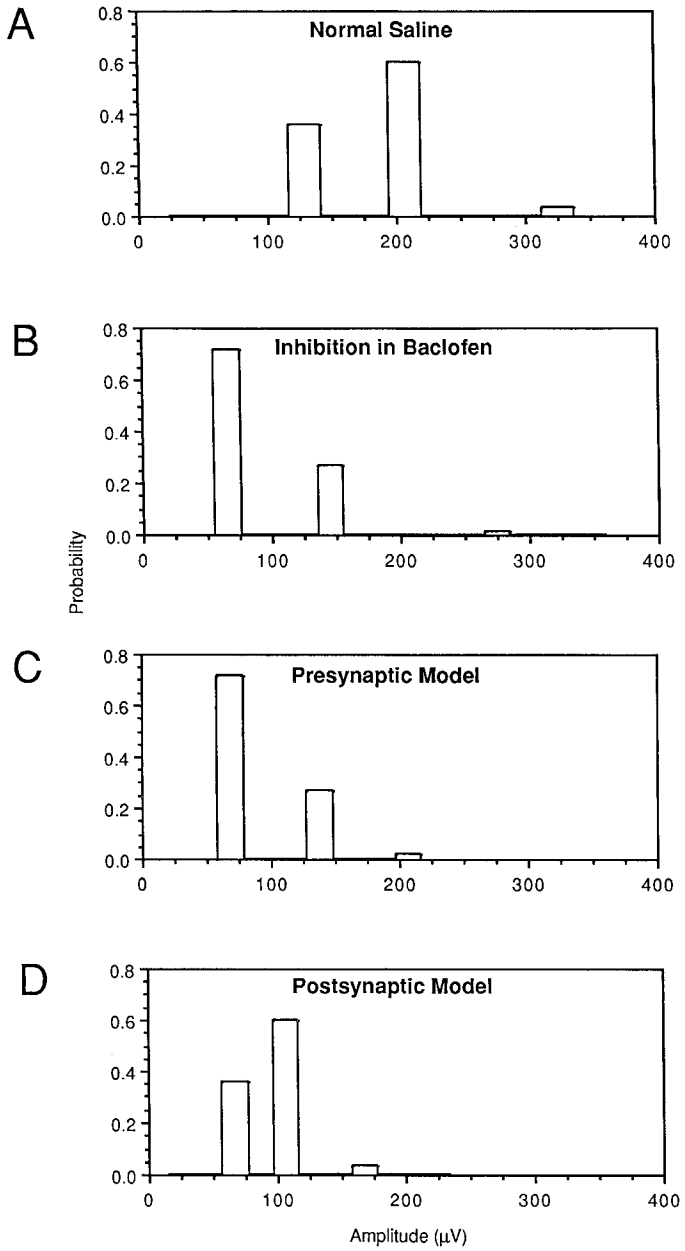

Figure 6. Quantal analysis of probability density functions of MUEPSPs in normal saline and in baclofen. The data are from unit s3 (Table 3). The distributions in *A* and *B* are taken directly from the deconvolutions as for Figures 1 and 5. The inhibition is then interpreted according to a presynaptic (*C*) or postsynaptic (*D*) model. For the presynaptic model, the quantal size was kept constant (the same as calculated from the distribution in *A*) and the number of 1, 2, and 3 quanta-responses was calculated to approximate the distribution in *B*. For the postsynaptic model, the quantal size was reduced by the amount of inhibition actually observed (ca. 50%), but the distribution of responses was kept the same as in *A*. For further details, refer to the text.

than 7%, and in the rest (10 units), it increased the halfwidths of the MUEPSPs by an average of 18.1%. The results of the last 10 units are consistent with the triceps-VRP measurements, where baclofen caused a small increase of the halfwidth. Taken together, these results show that baclofen produced little, if any, consistent increase in motoneuronal membrane conductance.

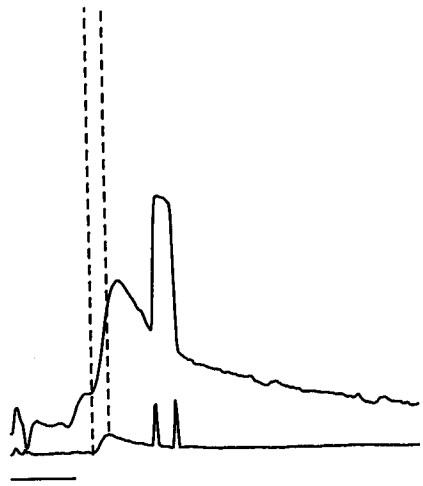

Figure 7. The electrical component of MUEPSPs does not fluctuate in amplitude. These traces, from unit b6 in normal saline, show the averaged MUEPSP (*upper trace*) and the SD of each point in this average (*middle trace*). The *dashed lines* indicate when the SD trace starts to rise and its peak. The calibration pulse on the MUEPSP is 0.5 mV and 3.7 msec at the base. The *bottom line* indicates the zero level for the SD trace.

Baclofen affected the quantal fluctuations of the MUEPSPs

Quantal analysis using the deconvolution procedure described in Materials and Methods was carried out for 4 units in a control study where only normal saline solution was used, 15 units in the present study and an additional 6 units for the study in the following paper. In all cases, the amplitudes of the pure MUEPSPs were clustered at discrete amplitudes. Furthermore, in most cases, the amplitude increments between any 2 adjacent nonzero bins were approximately the same. These observations provide strong evidence for quantal transmission at these synapses. The quantal size was therefore taken as the mean value of the increments between each 2 adjacent nonzero bins. This size was calculated for all the units analyzed, and they are listed in Table 3. Altogether, in 24 of the 25 units the averaged quantal size in normal saline ranged from 65 to 162 μV, with a mean value of 103 μV. In the remaining unit it was 260 μV.

To study the effects of baclofen on quantal fluctuations of the MUEPSPs, we carried out the deconvolution procedure for 15 of the 17 units where the SD of the noise was small enough and the sample size large enough for the results to be reliable. The results of deconvolutions for 4 of these units are shown in the histograms of Figures 5 and 6; results for all the units are listed in Table 3.

For 13 of the 15 units (all but b6 and s4), 5 μM baclofen reduced the probabilities for larger MUEPSPs to occur and increased those for smaller MUEPSPs. Moreover, the relative probabilities of the nonzero bins before and after superfusion of baclofen changed. These effects were reversed when baclofen was partially washed out in 4 of the 5 units (except unit s3) where the deconvolution procedure was performed for traces recorded during recovery. This suggests that baclofen caused presynaptic inhibition. The opposite result was obtained for unit b6, where in baclofen the probabilities for the larger MUEPSPs increased while those for the smaller ones decreased.

As reduction in quantal size is a good indicator for any concurrent involvement of postsynaptic inhibition, the average quantal size was calculated for each unit before and after the

application of baclofen. These values are listed in Table 3. Within the resolution of this method, in 13 of the 15 units (all but b2 and b5) the average quantal size stayed the same. Thus, the observed inhibition (except unit b6, in which the MUEPSP was augmented) in baclofen was largely due to a presynaptic mechanism, namely, the activation of $GABA_B$ receptors located on muscle afferents. For 13 of the 14 cases where baclofen induced inhibition, if there was any concurrent postsynaptic inhibition, it was below the resolving power of the method.

In 1 of the 15 units (b2), the MUEPSPs in baclofen had a reduced quantal size, a 51% decrease in halfwidth, and an increase in the slope of the initial part of their falling phase on the semilogarithm traces. Even for this unit, however, the 17% reduction in quantal size was not sufficient to account for the observed 40% reduction in MUEPSP amplitude. Therefore, for this unit at least half the inhibition caused by baclofen was still presynaptic.

Six of the units were chosen for more thorough analysis because they showed a sufficient amount of inhibition in baclofen to make a clear distinction between pre- and postsynaptic mechanisms and yet little enough so that the 2 probability density functions (in normal saline and baclofen) overlapped each other, which facilitates comparison between them. These units were b3, b4, m1, s2, s3, and s5. As described above, in all these cases, the quantal size remained the same within the limitation of the method. Moreover, the positions of the nonzero bins were reliable, as judged by their constancy of position when the deconvolution was run with several different bin shifts (see Materials and Methods). The synaptic responses fluctuated between the same discrete amplitudes in normal saline and in baclofen. This is to be expected if inhibition is the result of fewer quanta being released, but would not occur if the size of individual quanta were reduced.

An example of this is presented in Figure 6, which illustrates the analysis of unit s3. In the control histogram, the major peaks were separated by 77 μV. Since there was no measurable electrical component for this MUEPSP, this implies that the bin at 130 μV represents release of 2 quanta, and the peak at 207 μM represents release of 3 quanta. The actual data recorded in the presence of baclofen (shown in *B*) are completely compatible with the quantal sizes predicted from the control histogram (*A*) as shown in *C*. In contrast, if inhibition were mediated postsynaptically, the control histogram in *A* would be simply scaled to the left by 50% (the amount of inhibition observed) as shown in *D*. The resulting histogram is very different from the one actually observed. Similar results were obtained for the other 5 units; the results were always consistent with a presynaptic mechanism for inhibition but never with a postsynaptic one. These data therefore provide a strong argument that the major action of baclofen in reducing the amplitude of the MUEPSPs was mediated presynaptically.

Baclofen did not alter the potential changes occurring in sensory afferent terminals

The early electrical component of the MUEPSP reflects the depolarization of muscle afferent terminals by sensory impulses (Shapovalov et al., 1978; Shapovalov and Shiriaev, 1980; Westerfield and Frank, 1982). Barring changes in conductance of the motoneuronal membrane, these potentials can thus serve as a measure of the amplitude of the terminal depolarization. In contrast to the wide fluctuations in amplitude of the chemical component, the amplitude of the electrical component was virtually invariant both in normal saline and in baclofen. This can be seen most clearly in the traces in Figure 7, where the SD trace remains at the background noise level throughout the early electrical component of the MUEPSP and only begins to rise when the later chemically mediated component starts. A similar result is apparent in Figure 5*C* (for more examples, see Fig. 10 in Peng, 1988).

Table 4. Effects of 5 μM baclofen on the electrical MUEPSPs

Unit	Solution	Peaks (n)	Amplitude (μV)	σ_{MUEPSP} (μV)	σ_{noise} (μV)
b1	Saline	1	186	71.8	82.9
	Baclofen	1	172	86.6	86.1
b2	Saline	2	521	53.5	46.3
	Baclofen	1	375	61.6	55.4
b3	Saline	1	84	46.7	44.0
	Baclofen	1	102	39.2	40.8
	Saline	1	91	46.1	44.2
b6	Saline	1	114	50.4	50.4
	Baclofen	1	153	54.3	56.5
b7	Saline	1	176	74.4	71.7
	Baclofen	1	173	56.4	73.3
m2	Saline	1	161	52.1	49.5
	Baclofen	1	160	54.5	52.5
	Saline	1	155	61.8	62.0
m3	Saline	1	88	48.9	51.9
	1st baclofen	1	90	46.1	53.9
	2nd baclofen	1	65	70.9	62.3
s2	Saline	1	58	65.7	64.4
	1st baclofen	1	58	55.2	57.9
	2nd baclofen	1	63	59.8	60.4
	Saline	1	63	52.6	53.1

The possibility of conduction failure occurring in normal saline and in baclofen (which could thereby cause a reduction in the amplitude of afferent potential and hence presynaptic inhibition) was critically tested by analyzing the fluctuations of the electrical component of the MUEPSPs before and after the application of baclofen. For the 17 units studied for the effects of baclofen, 12 had a measurable electrical MUEPSP; the fluctuations of these components were studied in 8 units. The results are presented in Table 4.

In normal saline, the electrical MUEPSPs did not fluctuate in 7 of the 8 units; that is, the deconvolution resulted in a single peak. This is consistent with the fact that the SD of the electrical MUEPSP was the same as that of the noise. This was true for electrical MUEPSPs with amplitudes from 58 to 186 μV. For these units baclofen did not induce invasion failure because (1) the average amplitudes of the electrical MUEPSPs were not consistently or significantly changed and (2) there was no fluctuation in the amplitudes of the electrical MUEPSPs since the deconvolution resulted in a single nonzero bin for each of these units. These results imply that conduction failure is not likely to occur during normal transmission and that baclofen causes presynaptic inhibition via some mechanism(s) other than conduction failure.

One unit (b2) had an electrical component that behaved distinctly differently from the rest. In normal saline, the deconvolution procedure yielded 2 nonzero peaks at 493 and 543 μV,

each of which had a probability of about 0.5. Baclofen caused a 28% reduction in the average amplitude of the electrical MUEPSP and the deconvolution resulted in one component at 375 μV with a probability of 1. This single case is thus consistent with the possibility of branch point failure contributing to the observed inhibition of the chemical component.

Discussion

Activation of $GABA_B$ receptors inhibited the monosynaptic EPSPs

Baclofen, a specific $GABA_B$ receptor agonist, inhibited synaptic transmission between muscle sensory afferents and motoneurons. This was demonstrated by the reduction of the amplitude of both the monosynaptic component of the VRPs evoked by stimulating triceps nerves (or other muscle afferents) and the monosynaptic unitary EPSPs evoked by stimulation of single triceps sensory axons.

The amount of inhibition produced by baclofen was similar to that reported in other studies. We found that 5 μM baclofen reduced the peak amplitude of triceps-VRPs by an average of 47%. At comparable doses, baclofen was reported to cause a 50% inhibition of the monosynaptic EPSPs in rat hippocampal pyramidal cells (Lanthorn and Cotman, 1981).

The inhibitory effect of baclofen appeared to reach a plateau at 10 μM. Only 4 doses were tested, however, and the highest dose was 20 μM, so it is possible that the effect was not yet maximal. In fact, in cultured rat DRG cells, the additional inhibition of a Ca^{2+} current caused by raising the baclofen concentration from 10 to 25 μM was small (Dolphin and Scott, 1987), but a sharp increase occurred between 50 and 100 μM. Similarly, in cultured chick DRG cells the inhibitory effect of baclofen saturated at 100 μM (Dunlap, 1981). In any event, without a detailed knowledge of the transfer function at these synapses, a direct comparison of the dose–response relationship of baclofen is difficult, as we studied the effect of baclofen postsynaptically while the 2 studies cited above investigated presynaptic effects.

In contrast to the results reported here, Davidoff and Sears (1974) found that 100 μM baclofen had no effect on the monosynaptic component of the VRPs in the isolated frog spinal cord at 15°C. We have no explanation for the contradiction between these results and those of our own.

The inhibition caused by activation of $GABA_B$ receptors was presynaptic

Our study of the ventral root potentials showed that activation of $GABA_B$ receptors by baclofen reduced the amplitude of the triceps-VRPs with no apparent decrease in the membrane resistance of the motoneurons. This was confirmed by the study of the falling phase of the averaged intracellular MUEPSPs; for most of the MUEPSP units baclofen did not alter either the earlier or the later time constants of the decay of the potentials. For units b1 and b2, however, the initial part of the falling phase was more rapid in baclofen, while the later portions, reflecting the membrane time constants, remained unchanged. This might indicate the existence of postsynaptic inhibition occurring at distal dendrites. Alternatively, one could imagine that most of the synaptic sites were located near the recording site (most likely to be the soma), but a few were located on remote dendrites and gave rise to synaptic potentials in the soma only after the potentials resulted from the proximal synaptic currents had began to decay. If transmission at these remote sites were blocked, there would be an increased rate of fall in the initial part of the falling phase.

Similar to the results reported by Allan et al. (1980), Davidoff and Sears (1974), and Lev-Tov et al. (1988), we found that baclofen did not increase postsynaptic conductance. Either there are no $GABA_B$ receptors on spinal cord motoneurons or $GABA_B$ receptors on these motoneurons are not coupled to ionic channels that affect the resting conductance of these cells as in the case of some cortical and hippocampal neurons (Andrade et al., 1986; Howe et al., 1987). The limited studies reported here do not distinguish between these 2 possibilities.

Finally, quantal analysis of the fluctuations of the MUEPSPs demonstrated that baclofen inhibited these potentials by a reduction in quantal content rather than a reduction in quantal size. The recent results of Lev-Tov et al. (1988) concerning the effects of baclofen on posttetanic potentiation and depression of the monosynaptic EPSP in the cat spinal cord also provide evidence that baclofen causes presynaptic inhibition at these synapses.

Baclofen caused a small increase in the halfwidth of the VRPs, and in half of the MUEPSP units the absolute value of the slope of the falling phase on the semilogarithm traces was decreased slightly, suggesting an increase of the motoneuronal membrane resistance. This could be explained if baclofen inhibited release from the primary sensory afferent terminals, which in turn could reduce the amount of inhibitory transmitter being "spontaneously" released onto motoneurons from interneurons. This explanation might also apply to the slight hyperpolarization caused by baclofen recorded from the ventral root reported by others (Davidoff and Sears, 1974; Allan et al., 1980).

In contrast to the present findings, Fox et al. (1978) found that injection of baclofen caused a transient increase in membrane conductance of spinal motoneurons in cats. Furthermore, this increase could be blocked by bicuculline. A simple interpretation of these results is that baclofen can activate $GABA_A$ receptors to a significant extent. There is no other biochemical or electrophysiological evidence (Choi and Fischbach, 1981; Bowery et al., 1983; Simmonds, 1983) to support such an interpretation, however. Because of the complexity of neural pathways in the spinal cord, it is also possible to explain these results in terms of a polysynaptic $GABA_B$ receptor-mediated modulation of $GABA_A$ inputs to motoneurons.

Activation of $GABA_B$ receptors does not cause conduction failure in sensory afferents

The amplitude and time course of the population afferent potentials recorded from the ventral root were not changed by baclofen, nor was there any significant and consistent change in the amplitude of the electrical component of the MUEPSP recorded intracellularly from motoneurons. Furthermore, quantal analysis of the electrical component showed that baclofen did not cause this component to fluctuate. These observations make it likely that baclofen does not change the magnitude of the depolarization in sensory afferent terminals, nor does it cause conduction failure in some branches of the terminals, suggesting that baclofen interferes with release subsequent to depolarization of the terminal. Consistent with these findings, baclofen has been reported to have no effect on the action potentials invading presynaptic terminals in other systems (Fox et al., 1978; Lanthorn and Cotman, 1981; Dolphin and Scott, 1987).

In summary, activation of $GABA_B$ receptors can cause presynaptic inhibition at synapses between muscle afferents and spinal motoneurons in the frog. The presynaptic inhibition due to activation of $GABA_B$ receptors is unlikely to be the result of invasion failure of the potentials into the presynaptic terminals.

References

Allan, R. D., R. H. Evans, and G. A. R. Johnston (1980) γ-Aminobutyric acid agonists: An *in vitro* comparison between depression of spinal synaptic activity and depolarization of spinal root fibres in the rat. Br. J. Pharmacol. *70:* 609–615.

Andrade, R., R. C. Malenka, and R. A. Nicoll (1986) A G protein couples serotonin and $GABA_B$ receptors to the same channels in hippocampus. Science *234:* 1261–1265.

Barker, J. L., R. A. Nicoll, and A. Padjen (1975a) Studies on convulsants in the isolated frog spinal cord. I. An antagonism of amino acid responses. J. Physiol. (Lond.) *245:* 521–536.

Barker, J. L., R. A. Nicoll, and A. Padjen (1975b) Studies on convulsants in the isolated frog spinal cord. II. Effects on root potentials. J. Physiol. (Lond.) *245:* 537–548.

Barron, D. H., and B. H. C. Matthews (1938) The interaction of potential changes in the spinal cord. J. Physiol. (Lond.) *92:* 276–321.

Bormann, J., O. P. Hamill, and B. Sakmann (1987) Mechanism of anion permeation through channels gated by glycine and γ-aminobutyric acid in mouse cultured spinal neurones. J. Physiol. (Lond.) *385:* 243–286.

Bowery, N. G., D. R. Hill, and A. L. Hudson (1983) Characteristics of $GABA_B$ receptors binding sites on rat whole brain synaptic membranes. Br. J. Pharmacol. *78:* 191–206.

Burke, R. E., and P. Rudomin (1977) In *The Handbook of Physiology, Sect. 1: The Nervous System,* Vol. 1, pp. 877–944. Am. Physiol. Soc., Washington, D.C.

Choi, D. W., and G. D. Fischbach (1981) GABA conductance of chick spinal cord and dorsal root ganglion neurons in cell culture. J. Neurophysiol. *45:* 605–620.

Clements, J. D., I. D. Forsythe, and S. J. Redman (1987) Presynaptic inhibition of synaptic potentials evoked in cat spinal motoneurones by impulses in single group Ia axons. J. Physiol. (Lond.) *383:* 153–169.

Davidoff, R. A., and E. S. Sears (1974) The effects of lioresal on synaptic activity in the isolated spinal cord. Neurology *24:* 957–963.

Dolphin, A. C., and R. H. Scott (1987) Calcium channel currents and their inhibition by (−)-baclofen in rat sensory neurones: modulation by guanine nucleotides. J. Physiol. (Lond.) *386:* 1–17.

Dunlap, K. (1981) Two types of γ-aminobutyric acid receptor on embryonic sensory neurones. Br. J. Pharmacol. *74:* 579–585.

Eccles, J. C., R. M. Eccles, and F. Magni (1961) Central inhibitory action attributable to presynaptic depolarization produced by muscle afferent volleys. J. Physiol. (Lond.) *159:* 147–166.

Edwards, F. R., S. J. Redman, and B. Walmsley (1976) Statistical fluctuations in charge transfer at Ia synapses on spinal motoneurons. J. Physiol. (Lond.) *259:* 665–688.

Fletcher, R. (1970) A FORTRAN subroutine for general quadratic programming. UKAEA Res. Group Rep., AERE R. 6370.

Fletcher, R. (1971) A general quadratic programming algorithm. J. Inst. Math. Appl. *7:* 76–91.

Fox, S., K. Krnjevic, M. E. Morris, E. Puil, and R. Werman (1978) Action of baclofen on mammalian synaptic transmission. Neuroscience *3:* 495–515.

Frank, E., and M. Westerfield (1982) Synaptic organization of sensory and motoneurons innervating triceps brachii muscles in the bullfrog. J. Physiol. (Lond.) *324:* 479–494.

Frank, K., and M. G. F. Fuortes (1957) Presynaptic and postsynaptic inhibition of monosynaptic reflexes. Fed. Proc. Fed. Am. Soc. Exp. Biol. *16:* 39–40.

Gahwiler, B. H., and D. A. Brown (1985) $GABA_B$-receptor-activated K^+ current in voltage-clamped CA_3 pyramidal cells in hippocampal cultures. Proc. Natl. Acad. Sci. USA *82:* 1558–1562.

Gasser, H. S., and H. T. Graham (1933) Potential produced in the spinal cord by stimulation of dorsal roots. Am. J. Physiol. *103:* 303–320.

Hays, W. (1973) *Statistics for the Social Sciences,* 2nd ed. Holt, Rinehart and Winston, New York.

Hosmer, D. W. (1978) Comment on Quandt and Ramsey's paper. J. Am. Stat. Assoc. *73:* 741–744.

Howe, J. R., B. Sutor, and W. Ziegagansberger (1987) Baclofen reduces post-synaptic potentials of rat cortical neurones by an action other than its hyperpolarizing action. J. Physiol. (Lond.) *384:* 539–569.

Hughes, J., and H. S. Gasser (1934) Some properties of the cord potentials evoked by a single afferent volley. Am. J. Physiol. *108:* 307–321.

Lanthorn, T. H., and C. W. Cotman (1981) Baclofen selectively inhibits excitatory synaptic transmission in the hippocampus. Brain Res. *225:* 171–178.

Lev-Tov, A., D. E. R. Meyers, and R. E. Burke (1988) Activation of type B γ-aminobutyric acid receptors in the intact mammalian spinal cord mimics the effects of reduced presynaptic Ca^{+2} influx. Proc. Natl. Acad. Sci. USA *85:* 5330–5334.

Lichtman, J. W., and E. Frank (1984) Physiological evidence for specificity of synaptic connections between individual sensory and motor neurons in the brachial spinal cord of the bullfrog. J. Neurosci. *4:* 1745–1753.

Ling, L., and D. J. Tolhurst (1983) Recovering the parameters of finite mixtures of normal distributions from a noisy record: An empirical comparison of different estimating procedures. J. Neurosci. Methods *8:* 309–333.

Massey, F. J., Jr. (1951) The Kolmogorov-Smirnov test for goodness of fit. Am. Stat. Assoc. *46:* 68–78.

Nicoll, R. A., and B. E. Alger (1979) Presynaptic inhibition: Transmitter and ionic mechanisms. Int. Rev. Neurobiol. *21:* 217–258.

Peng, Y. (1988) *Functional roles of $GABA_A$ and $GABA_B$ receptors in synaptic transmission between the muscle spindle afferents and motoneurons in bullfrog spinal cord.* Ph.D. dissertation, Northwestern University, Evanston, IL.

Potashner, S. J. (1978) Baclofen: Effects on amino acid release. Can. J. Physiol. Pharmacol. *56:* 150–154.

Rall, W. (1969) Time constants and electrotonic length of membrane cylinders and neurons. Biophys. J. *9:* 1483–1508.

Schofield, P. R., M. G. Darlison, N. Fujita, D. R. Burt, F. A. Stephenson, H. Rodriguez, L. M. Rhee, J. Ramachandran, V. Reale, T. A. Glencorse, P. H. Seeburg, and E. A. Barnard (1987) Sequence and functional expression of the $GABA_A$ receptors shows a ligand-gated receptor super-family. Nature *328:* 221–227.

Shapovalov, A. I., and B. I. Shiriaev (1980) Dual mode of junctional transmission at synapses between single primary afferent fibres and motoneurons in the amphibian. J. Physiol. (Lond.) *306:* 1–15.

Shapovalov, A. I., B. I. Shiriaev, and A. A. Velumian (1978) Mechanisms of post-synaptic excitation in amphibian motoneurones. J. Physiol. (Lond.) *279:* 437–455.

Shreider, Y. A. (1966) *The Monte Carlo Method. The Method of Statistical Trials,* Pergamon, Oxford, UK.

Simmonds, M. A. (1983) Multiple GABA receptors and associated regulatory sites. TINS *6:* 279–281.

Smirnov, N. (1948) Table for estimating the goodness of fit of empirical distributions. Ann. Math. Stat. *19:* 279–281.

Westerfield, M., and E. Frank (1982) Specificity of electrical coupling among neurons innervating forelimb muscles of the adult bullfrog. J. Neurophysiol. *48:* 904–913.

Wong, K., and S. Redman (1980) The recovery of a random variable from a noisy record with applications to the study of fluctuations in synaptic potentials. J. Neurosci. Methods *2:* 389–409.